

P2.2 REDUCING THE IMPACT OF NOISE ABATEMENT PRACTICES ON AIRPORT CAPACITY BY FORECASTING SITUATIONAL DEPENDENT AIRCRAFT NOISE PROPAGATION

R. Sharman* and T. Keller
Research Applications Program
National Center for Atmospheric Research
Boulder, CO

ABSTRACT

In attempts to reduce population exposure to aircraft noise near large airports, current approach and departure routes have been developed based upon population analyses and static meteorological climatologies as implemented for example in the FAA Integrated Noise Model (INM). However, commercial aircraft have noise “footprints” that are determined not only by the operational configuration of the aircraft but also by the highly variable atmospheric environment through which the sound is propagating. The existing approach and departure routes do not reflect these dynamically changing patterns of noise dispersion and propagation.

This paper attempts to quantify the influence of meteorological variability on the shape and extent of aircraft acoustic footprints by using a sound propagation model to predict the acoustic propagation patterns. Both idealized meteorological profiles and actual profiles from soundings are used in the evaluation. For the cases examined, the acoustic footprint is usually smaller than that predicted by the INM, but can also be substantially larger in particular directions around the aircraft due to sound channeling by low level wind shears. With the combined use of a sound model and meteorological measurements and/or forecasts it may be possible to develop runway use strategies to minimize population exposure to aircraft noise while reducing the adverse effects of noise abatement procedures on airport operations.

1. Introduction

Current approach and departure routes at a number of airports reflect attempts to balance

flight operations and population densities to achieve noise abatement objectives. However, the patterns of noise propagation and dispersion depend strongly on the variability of the weather. In contrast, most current noise abatement constraints on airport departure routes are virtually constant for all meteorological conditions. They do not vary with the weather, and this may present a potential opportunity to enhance airport capacity.

This study is an attempt to quantify the effect of the meteorological variability on sound propagation from aircraft and consequent sound levels experienced at the surface. Both idealized meteorological profiles and actual profiles from soundings are examined. In either case, the meteorological profile is input to a general use sound propagation model known as the fast field program (FFP). This is a quasi two-dimensional, single frequency model that was originally developed for predicting sound propagation in the ocean. It has been extended to atmospheric applications as well (Lee et. al., 1986, Franke and Swenson, 1989, Noble and Marlin, 1995). With the aircraft modeled as a single frequency source at various flight levels in the atmosphere, the FFP derives the sound propagation pattern in a vertical plane at a particular azimuth from the source, taking into account spherical spreading, molecular absorption, refraction, and surface interactions. By considering a full range of azimuths (as in Figure 1), a two-dimensional plot of sound levels in a horizontal plane surrounding the source and containing the receiver may be constructed. Further, if the spectral content of sound generated by a particular aircraft is known, the model can be run with different frequencies, and the results A weighted to give the sound level at the receiver. A-weighting is often used to give a better representation of the sound as a human observer would perceive it (e.g., Pierce, 1989). Alternatively, the effect of atmospheric variability

*Corresponding author address:

sharman@ucar.edu

can be examined by simply looking at one individual frequency representative of the aircraft.

In an attempt to quantify the source levels in a realistic manner, the intensity of the source is derived from an example given in Appendix E of the SAE standard for airplane noise prediction (SAE AIR 1845, 1986). In that appendix sound levels are derived for a hypothetical two-engine jet aircraft on departure. Noise-power-distance (NPD) data is given, and that data, for the hypothetical takeoff configuration at brake release, is used to normalize the sound levels computed from the FFP. The sound level pattern derived from the SAE Standard algorithms (which are implemented in the FAA INM) for this example is shown in Figure 2. In this and all subsequent figures, sound patterns are shown as colored contour plots of sound levels in dB, at the receiver height of 1.2 m, over a two kilometer area with the source (prescribed at 10 m elevation) at the center of the figure. A color bar along the upper right of the figure can be used to quantify the levels in the pattern. In the figure, the standard adjustments for duration and directivity have not been included, since these effects are not modeled in the FFP. Note the completely symmetric (in azimuth) structure of both patterns, and that the 80 dB level is at a radial distance of about 1 km.

In the next two sections this pattern will be compared and contrasted with patterns derived from the FFP using first, idealized meteorological profiles, and second, actual meteorological profiles gathered from one year's worth (1998) of sounding data from Upton NY, USA. Upton is a designated World Meteorological Organization (WMO) sounding station, and was chosen for its relatively close proximity to JFK International Airport (about 80 km east). Soundings are taken there routinely twice daily, at 0 UTC and 12 UTC, so this represents over 700 sample atmospheric structures.

2. Results with ideal atmospheric structures

To better interpret results using the FFP with the actual sounding data from Upton, it is instructive to first consider some idealized atmospheric profiles. The obvious first case to examine is the vertical structure corresponding to a "standard atmosphere." The standard atmosphere actually has a precise definition in terms of pressure, temperature, and density profiles (e.g., U.S. Standard Atmosphere, 1966). However winds and humidity are not specified. Here the dry, standard atmosphere is used with

the SAE standard prescribed headwind of 4 m/s and dry air for noise calculations. Figure 3 shows the FFP sound pattern produced for a dry, standard atmosphere with an east wind of 4 m/s, and for three different source frequencies, 100, 1000, 10000 Hz. The patterns are azimuthally symmetric and, because the effect of molecular absorption is frequency dependent, the radius of the pattern increases as the frequency decreases.

In order to compare the FFP derived sound level patterns to the pattern computed from the SAE standard in Figure 2, this case was also integrated over frequency and A weighted. Although a precise comparison is not possible since the spectral distribution of noise from the hypothetical two engine aircraft was not given in the standard, using two-engine spectral class data from the INM (see FAA DTS-34-FA065-LR1, 1999) should give a reasonable comparison. The data for INM spectral departure class 102 (see Figure 4) was used together with A weighting of the frequency dependent response output from the FFP to derive the pattern shown in Figure 5. Note that the overall pattern is similar to that in Figure 2 although the radial distribution is different, and the pattern somewhat smaller in size than the 1000 Hz pattern shown in Figure 3b.

These patterns are all symmetric, or nearly so, since the effect of temperature gradients acts the same in all propagation directions, and the wind speed is generally much smaller than the speed of sound. But if wind shear (viz., the vertical shear of the horizontal wind) is introduced, an azimuthal dependence will appear for a favorable alignment of wind direction and shear magnitude. This is demonstrated in the pattern shown in Figure 6 for an east wind increasing with height, but otherwise the conditions are the same as those used to construct Figure 3b (i.e., 1000 Hz source and a standard atmosphere). Figure 6a is the result obtained for a small shear of .01 m/sec/m and shows the pattern is expanded slightly to the left (west). Figure 6b shows the result obtained with a larger value of shear of .25 m/sec/m. Here the symmetry is almost entirely destroyed, with propagation dominantly to the west and taking on a bell-shaped pattern in the left half of the diagram. Reflection from the surface and refraction aloft causes a reinforcement of the intensity near the left boundary of the figure. The pattern in the right half of the figure (to the east of the source) is still fairly uniform, but the influence is somewhat smaller than in the no shear case. These bell-shaped patterns are obtained in more general cases with shear vectors

rotating with increasing height, as will be demonstrated in the next section.

3. Results with actual atmospheric structures

As mentioned in the introduction, in order to gain an appreciation of the extent of day-to-day variability in sound levels due to varying meteorological conditions, the actual twice daily sounding data for Upton NY was used as input to the FFP. For the sample sounding the east and west components of the wind were decomposed into components parallel and normal to each radial plane computed by the FFP. In each plane, wind shear is computed only from the component tangent to the plane. A sample of resulting patterns for a 1000 Hz source is shown in Figure 7. Because substantial wind shears are usually present in the lower atmosphere, the sound propagation patterns rarely look like that derived from the standard atmosphere with constant wind, and instead show the bell-shaped pattern indicative of favorable horizontal propagation in certain azimuthal directions. These patterns occur regardless of the season and time of day. If these patterns were averaged over all samples from the year, it is probable that the pattern would be roughly symmetric, and be about the same size as the INM example in Figure 2.

The effect of elevating the source is shown in Fig. 8. An actual sounding taken at Upton at 1200UTC on 7 July 1999 (Fig. 8) was used as an input to the FFP model. The source spectrum was as shown in Fig. 4, A-weighted and normalized in the same manner as was used in Fig. 5. The FFP-derived sound levels at a receiver height of 1.2m for four different source heights are shown in Figure 9. The northwesterly wind at the surface causes the propagation pattern to be stretched “downstream” to the southeast at lower levels. At upper levels the pattern becomes more symmetric, especially above about 300m where the low level wind shear ceases and can therefore no longer trap the sound near the surface. Of course the sound level intensity decreases as the source to receiver distance increases.

4. Forecasting sound levels using numerical weather prediction model output

In the previous sections it was demonstrated that the sound propagation patterns from aircraft depend strongly on the vertical distribution of low level wind and temperature. The atmospheric structure may be obtained in real time by rawinsondes or wind profiler measurement in the

vicinity of the airport, or possibly from profiles derived from local numerical weather prediction (NWP) model analyses. It would of course be beneficial to be able to *predict* sound levels so that particularly offensive patterns and consequent noise complaints could be minimized by adjusting approach and departure routes. The procedure would be to extract environmental profiles from NWP forecast models and use these profiles in a sound propagation model such as the FFP, to predict sound levels associated with various aircraft types. To test the feasibility of this approach we retrieved soundings in the vicinity of Upton, NY from 6 hour Rapid Update Cycle (RUC) (see Benjamin et al., 2004) forecasts and used the FFP to compute sound propagation patterns at the surface. We then compared the FFP solution derived from the RUC forecast to the FFP solutions based on the actual Upton sounding for the time of the forecast. Two examples are provided in Fig. 10. In both cases the RUC 6-hr forecast provides correct information about the azimuthal dependence of the sound propagation pattern, but in each case the radial distribution suffers in the forecast. Overall, the implication from our results though is that coupled NWP-sound propagation models may have enough skill to be useful in daily approach and departure planning strategies. As NWP model resolution and accuracy increases, more reliable sound propagation forecasts will follow.

5. Summary and conclusions

This preliminary look at the effect of atmospheric variability on aircraft sound propagation has shown that:

- (1) The sound propagation footprint emanating from an aircraft undergoes substantial diurnal and day-to-day variability, both in the size of the footprint, and in the azimuthal variations;
- (2) The azimuthal variations are due mainly to low level wind shear.
- (3) The INM standard agrees well with the results of a sophisticated sound model only in the case of no winds and a standard atmosphere.
- (4) However, under conditions other the standard atmosphere the substantial variations noted above may cause the actual noise levels at the surface to deviate dramatically from the standard in certain directions.
- (5) Sound levels could be *nowcast* using soundings or other measurements to provide the atmospheric vertical structure, which in turn could be used to drive a sound propagation model

to derive the three-dimensional sound level pattern.

(5) It may be also be possible to use coupled NWP forecasts with sound propagation models to *forecast* sound levels of approaching and departing aircraft several hours in advance.

The generality of these results needs to be substantiated with more systematic case studies, and especially with measurements of sound level near the surface for verification. In the likely event that the results presented here are more generally applicable, this suggests strategies that may be invoked in future airport planning and operations that may increase airport capacity by taking advantage of days/times when the sound propagation is minimal. For example, if an aircraft is departing from an east coast terminal which is close to the coast, during times when the environmental conditions throw the sound pattern over the water, a takeoff heading could be chosen that would minimize exposure to population areas over the land. Other scenarios could be envisioned. If the coupled forecast models had sufficient predictive skill the noise forecasts could be used to select the most efficient approach and/or departure routes by simulating the operational impact of alternative routing strategies at airports, and to minimize population exposure to aircraft noise. In this way it may be possible to attain significant reductions in the number of flight operations constrained by noise abatement procedures, without increasing the population exposure to aircraft noise.

REFERENCES

Benjamin, S.G., G.A. Grell, J.M. Brown, T.G. Smirnova, and R. Bleck, 2004: Mesoscale weather prediction with the RUC hybrid isentropic-terrain-following coordinate model. *Mon. Wea. Rev.*, **132**, 473-494.

Franke, S. J. and G. W. Swenson, Jr., 1989: A brief tutorial on the Fast Field Program (FFP) as applied to sound propagation in the air. *Applied Acoustics*, **27**, 203-215.

Lee, S. W., N. Bong, W.F. Richards, and R. Raspet, 1986: Impedance formulation of the fast field program for acoustic wave propagation in the atmosphere. *J. Acoust. Soc. Am.*, **79**, 628-634.

Noble, J. M. and D. Marlin, 1995: *User's manual for the Scanning Fast Field Program (SCAFFIP) general version 1.0*. Army Research Laboratory ARL-TR-545, 129 pp.

Pierce, A. D., 1989: *Acoustics, An introduction to its physical principles and applications*. Acoustical Society of America, New York, 678 pp.

U.S. Department of Transportation, 1999: *Spectral classes for FAA's Integrated Noise Model version 6.0*. DTS-34-FA065-LR1.

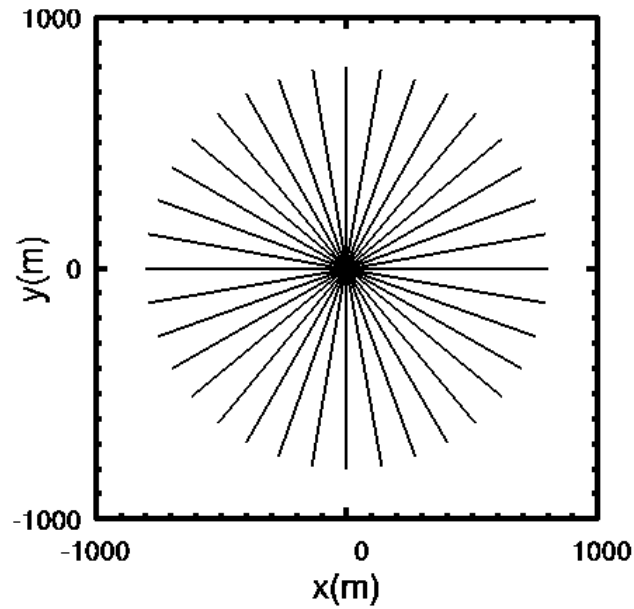


Figure 1. Azimuthal placement of radials used in the FFP computations. Azimuthal increment is 10 degrees. The source is assumed to be at the center ($x=y=0$). Sound levels are computed along each radial separately and the resulting pattern is contoured in this x-y plane.

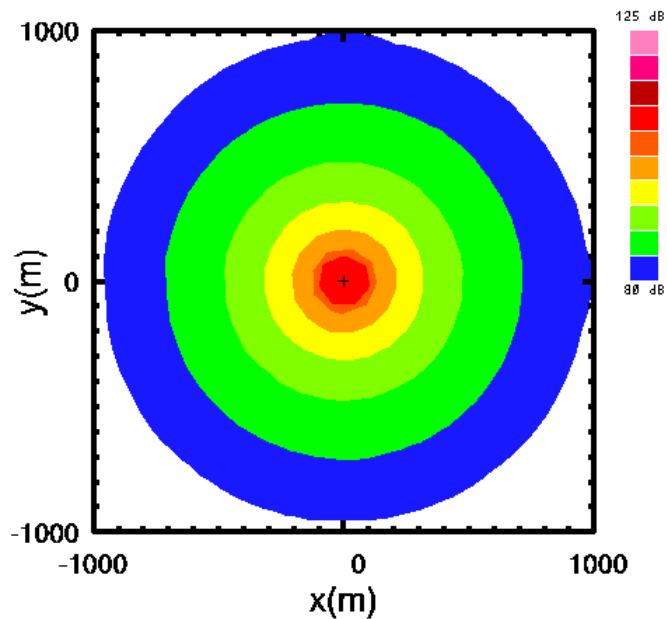


Figure 2. Sound level pattern as computed from SAE AIR 1845 algorithms for a hypothetical two engine aircraft at 10 m elevation and a receiver at 1.2 m elevation. The parameters used in this computation were taken from the NDP curves in Appendix E of the Standard. Directivity and duration effects were not included.

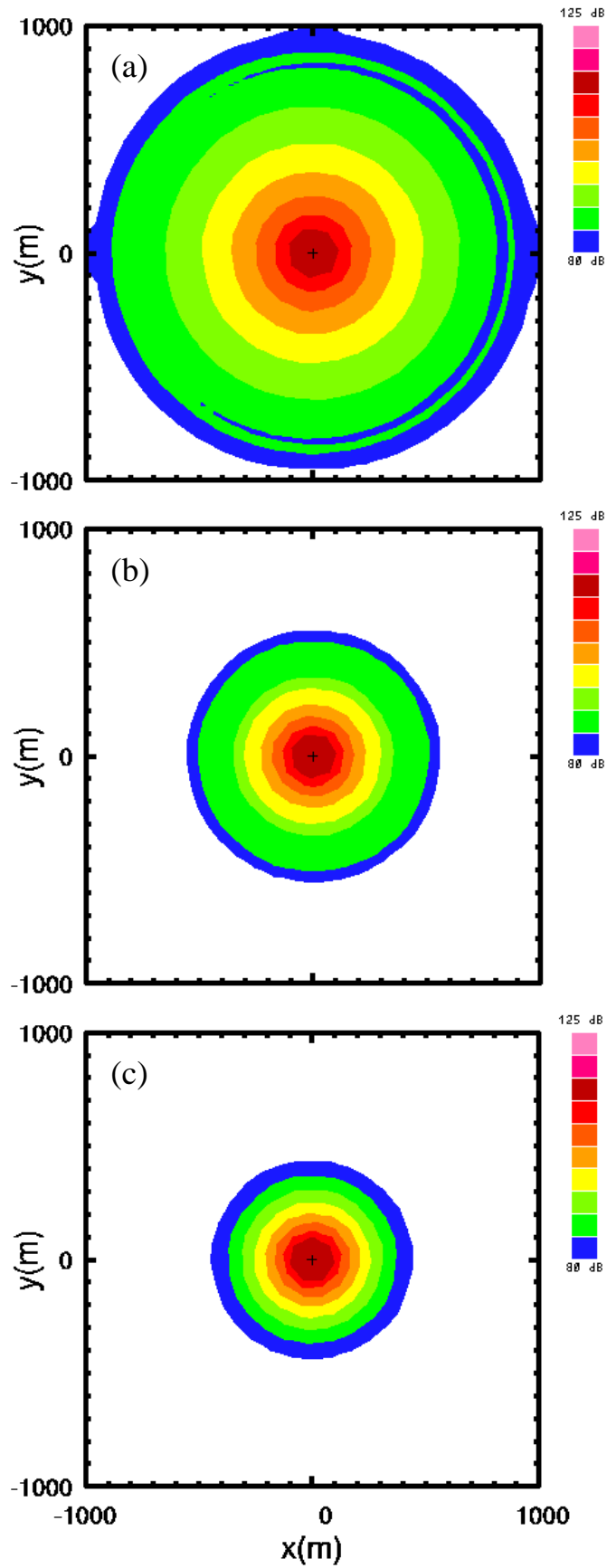


Figure 3. FFP derived patterns for a standard dry atmosphere and a 5 m/s east wind for a source frequency of (a) 100 Hz, (b) 1000 Hz, and (c) 10,000 Hz.

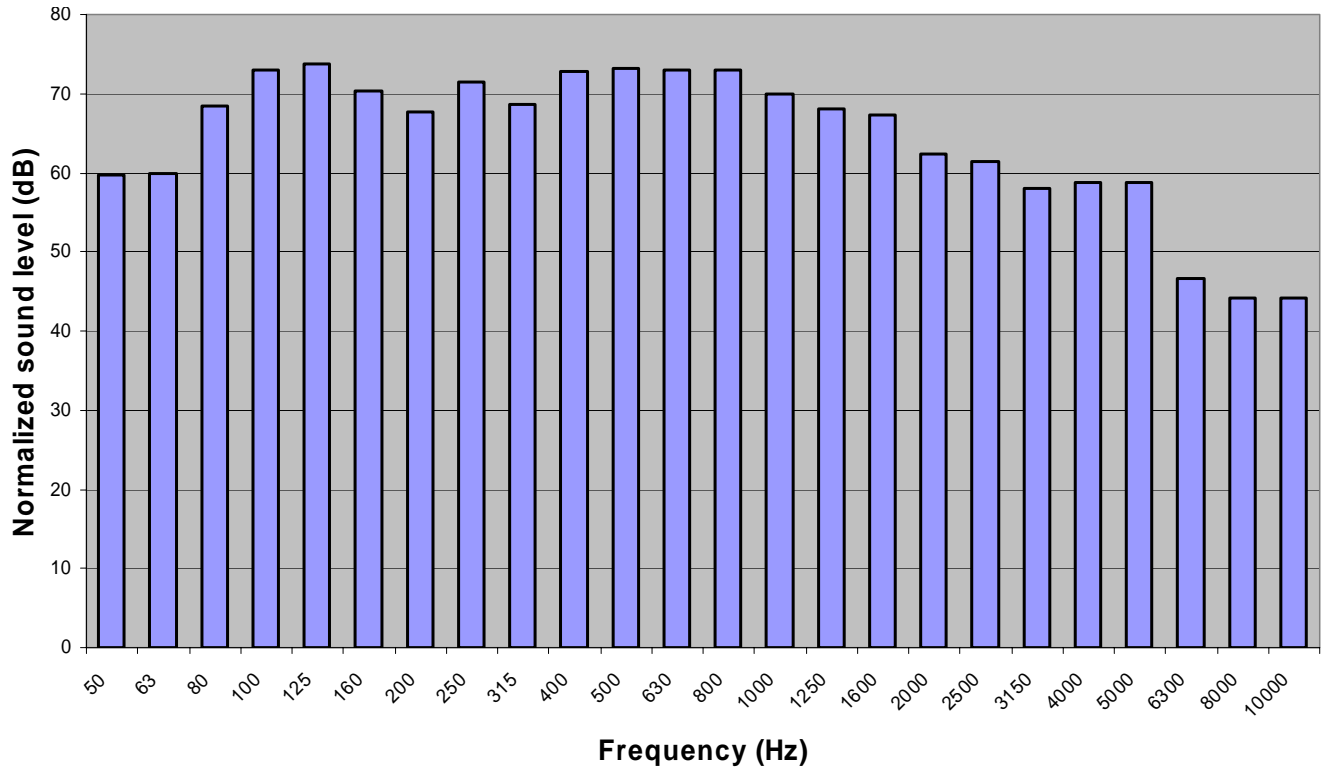


Figure 4. Source spectrum for INM departure spectral class 102, typical of B737 commercial carriers.

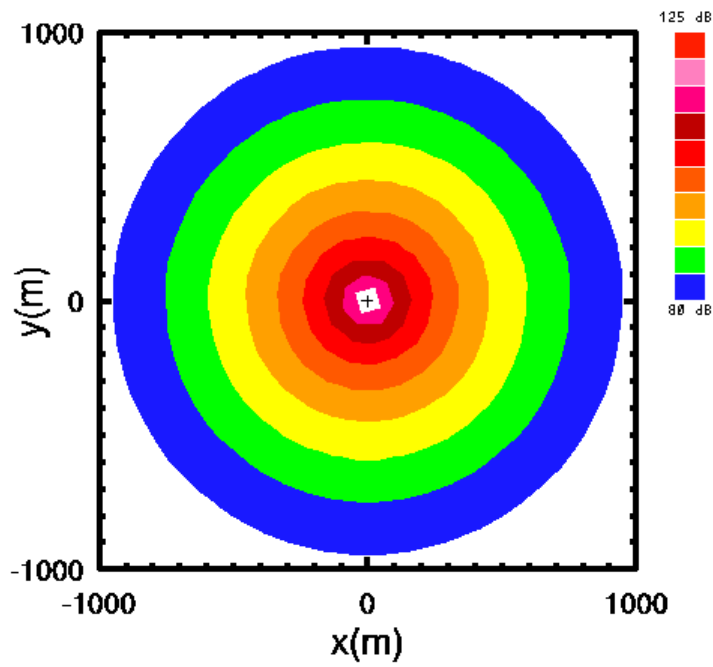


Figure 5. FFP derived sound levels using A weighting and a spectral distribution of source frequency amplitudes specified by INM spectral class 102 (Fig. 4).

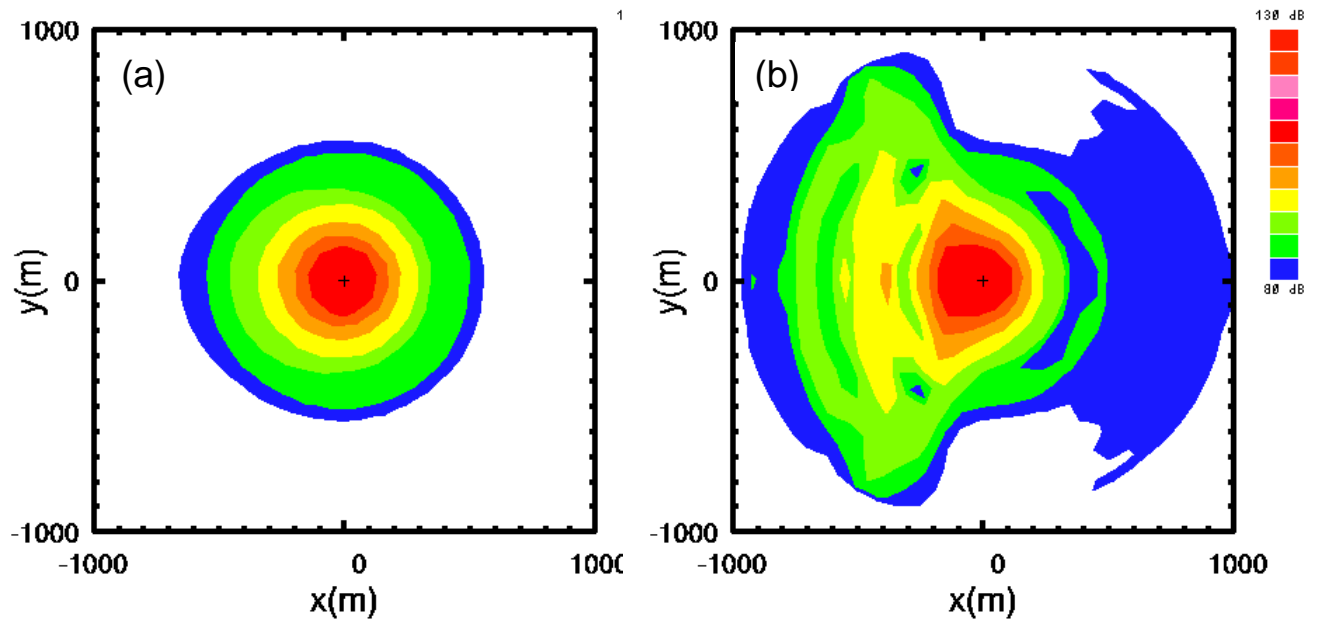


Figure 6. FFP derived sound propagation patterns computed for a 1000 Hz source in a standard atmosphere and with a wind shear of (a) .01 /sec, and (b) .25 /sec.

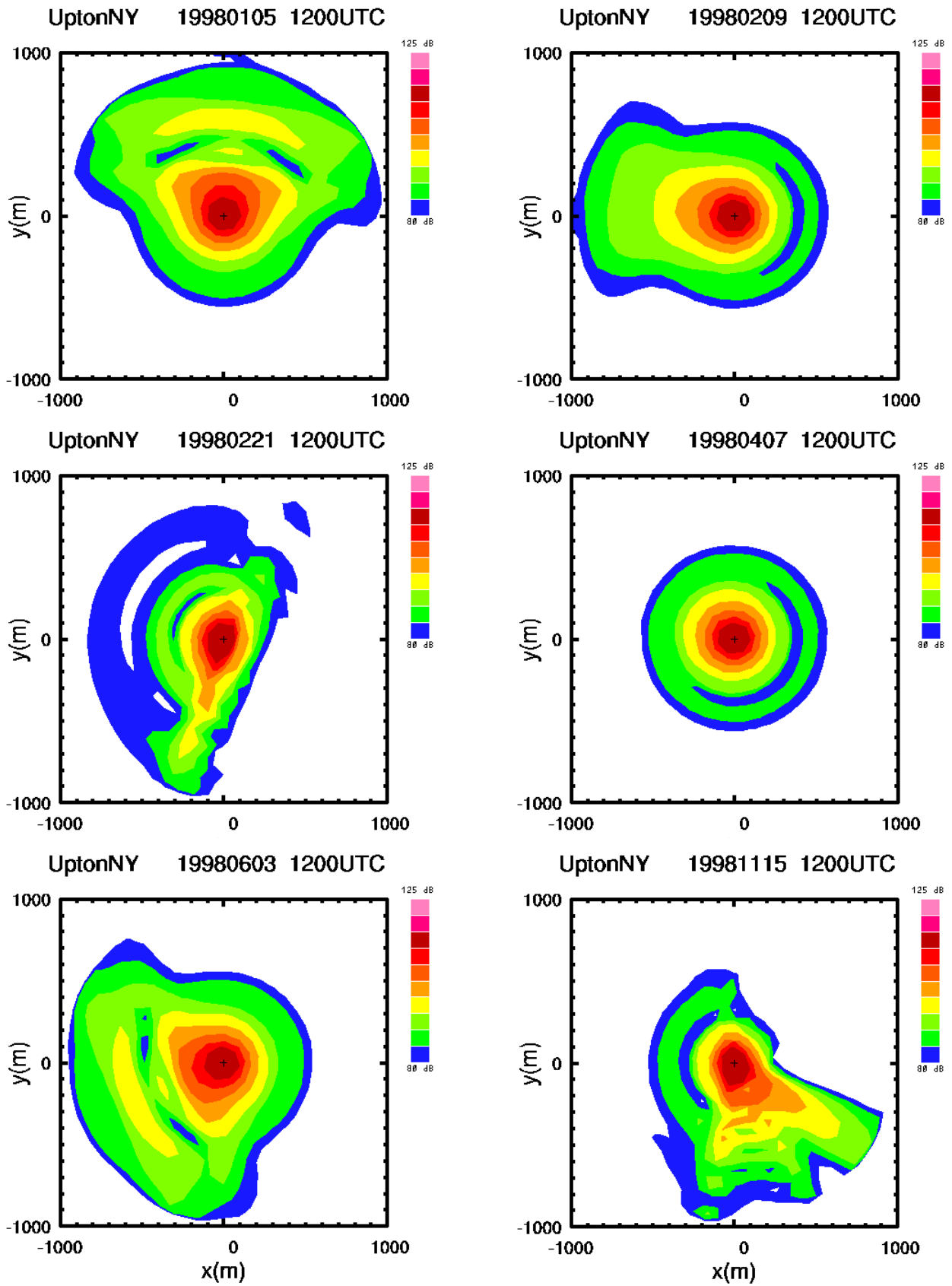


Figure 7. Six different FFP computed sound patterns for a source of frequency 1000 Hz and using six different input soundings from Upton NY for the dates/times indicated.

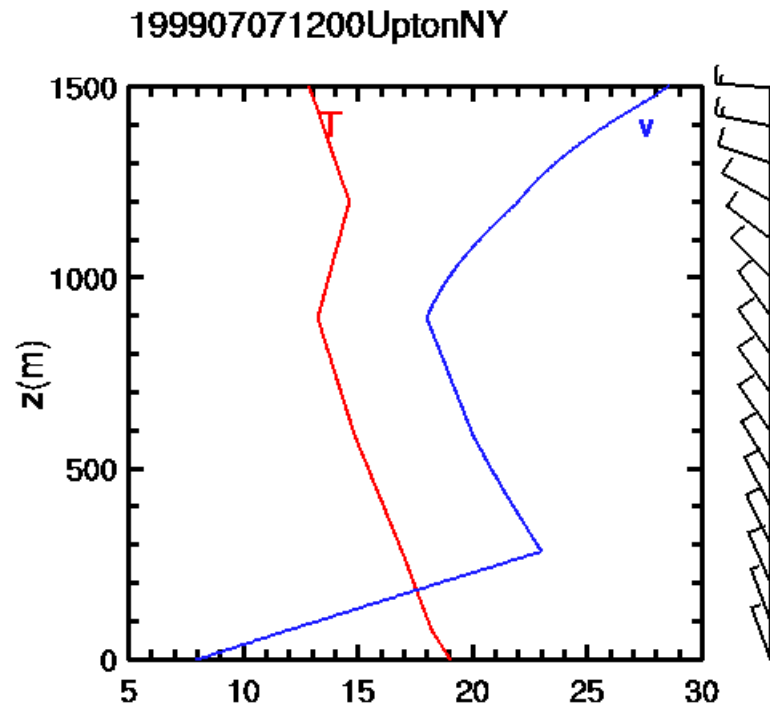


Figure 8. Sounding in the lowest 1500 m taken at Upton NY, 7 July 1999 at 1200UTC. Temperature profile is drawn in red, the speed profile in blue. Wind barbs to the left can be used to infer wind direction and directional shear.

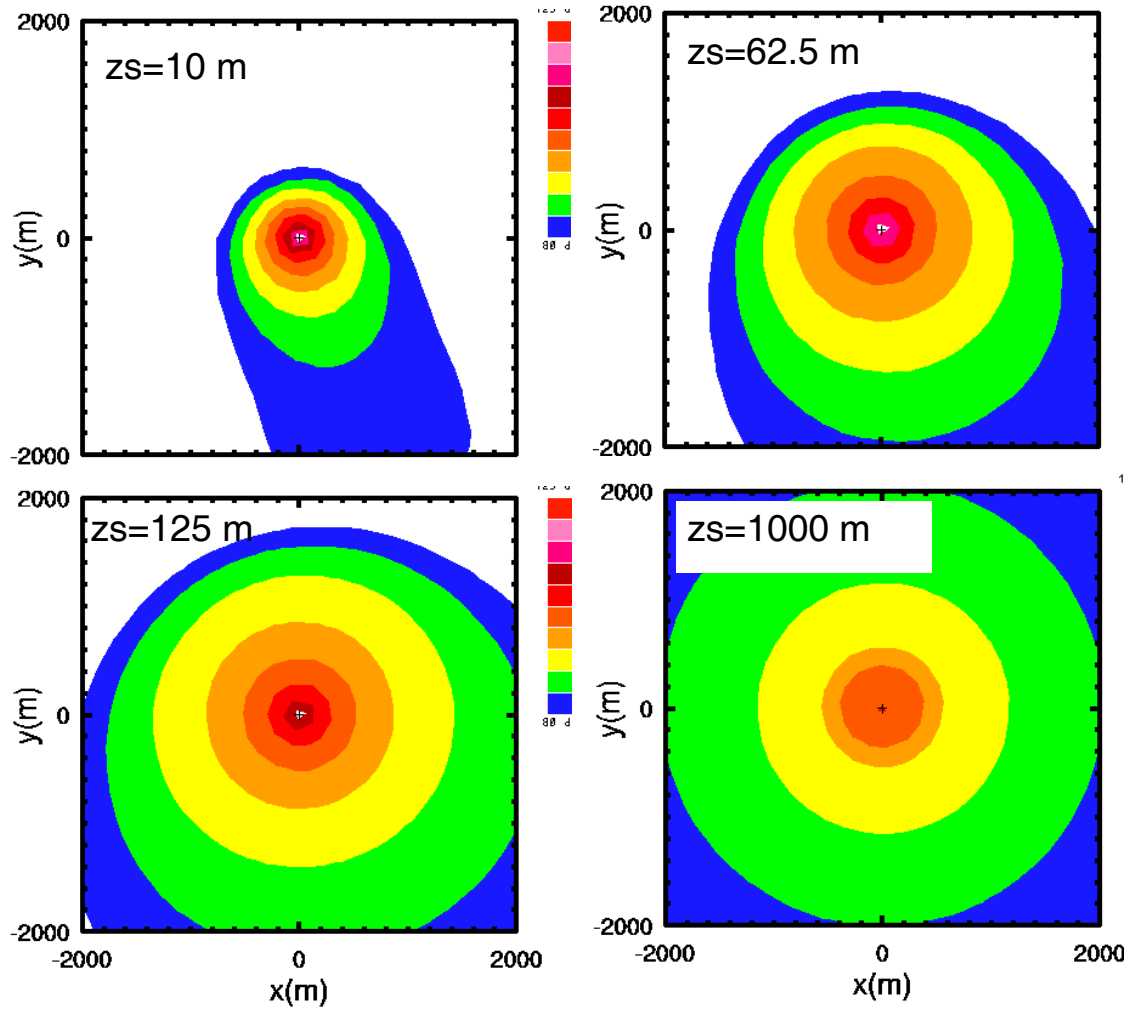


Figure 9. A-weighted FFP derived sound levels near the surface (1.2m) for four different source elevations z_s , assuming a hypothetical two-engine aircraft at takeoff, climbing through the atmospheric profile shown in Fig. 8.

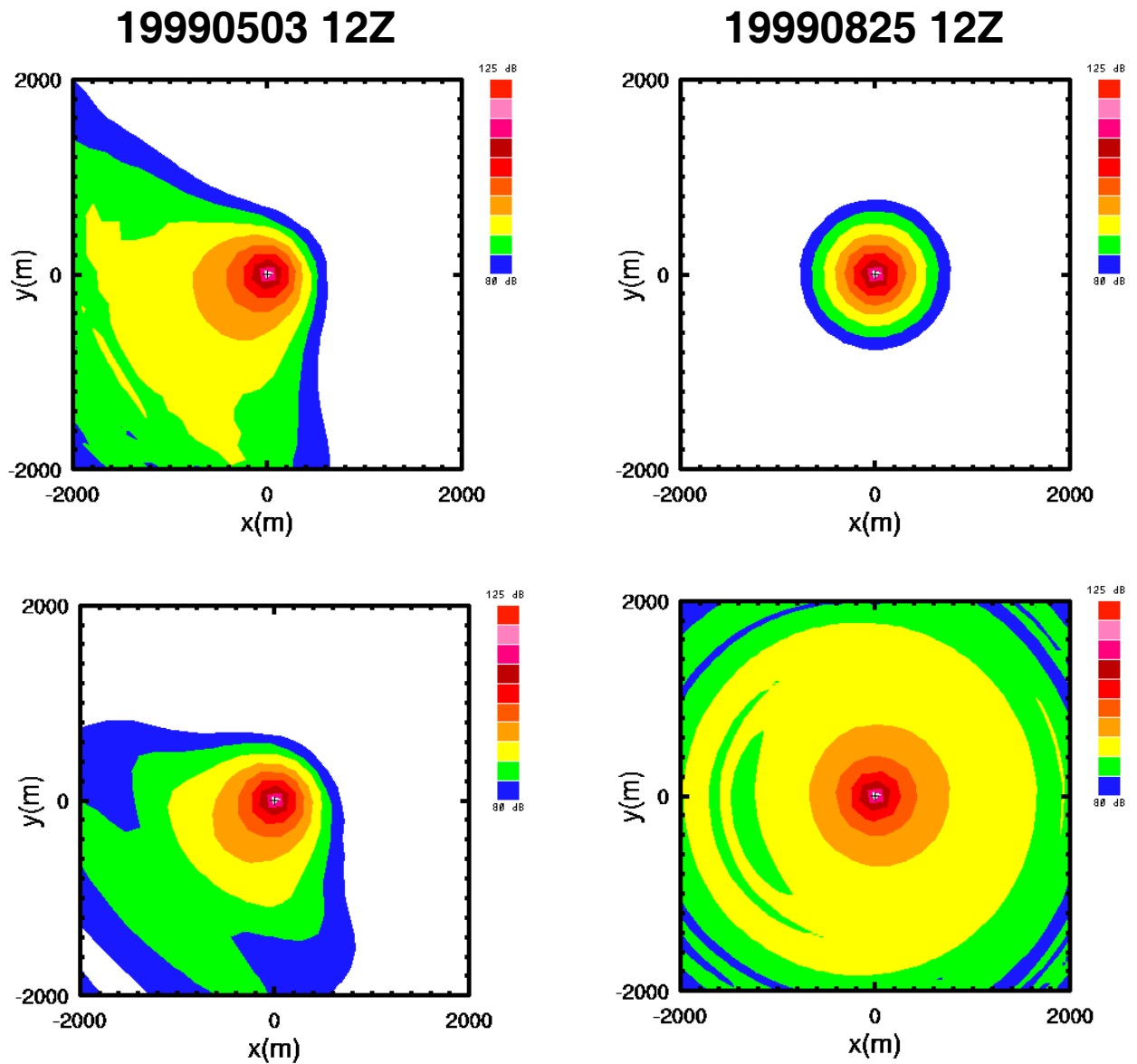


Figure 10. Comparison of FFP-derived sound levels near the surface for a source at 10 m elevation based on Upton, NY rawinsonde profiles (upper panels) and RUC 6hr forecasts valid at the same time using the nearest grid point to Upton to derive the sounding (lower panels). Two examples are shown, 3 May 1999 1200UTC (left panels) and 25 Aug 1999 1200 UTC (right panels).